Chemical Methodologies 10(2026) 514-528

Chemical Methodologies

Journal homepage: http://chemmethod.com

Original Article

High-Performance PES Membranes Prepared by VNIPS: Role of Brij-58 in Enhancing Surface Hydrophilicity and Antifouling Resistance

Miftahul Arzaq[1], Muhammad Az-Harry[1], Haziqia Aulia Putri[1], Nasywa Humaira Nasrul[2], Sri Mulyati[1,3], Cut Meurah Rosnelly[1,3], Nafiu Umar Barambu[1], Muhammad Prayogie Aulia[4], Nasrul Arahman[1,3,5]*

[1]*Department of Chemical Engineering, Universitas Syiah Kuala, Banda Aceh 23111, Indonesia*
[2]*Department of Pharmacy, Universitas Syiah Kuala, Banda Aceh 23111, Indonesia*
[3]*Graduate School of Environmental Management, Universitas Syiah Kuala, Jl. Tgk Chik Pante Kulu No. 5, Banda Aceh 23111, Darussalam, Indonesia*
[4]*Department of Chemical Engineering, Kobe University, Nada-Ku Hyogo, Japan*
[5]*Atsiri Research Center, Universitas Syiah Kuala, Jl. Syeh A. Rauf, Darussalam, Banda Aceh 23111, Indonesia*

ARTICLEINFO

Article history
Submitted: 2025-11-30
Revised: 2025-12-28
Accepted: 2026-01-30
ID: CHEMM-2511-2051

DOI: 10.48309/chemm.2026.562772.2051

KEYWORDS
Antifouling
Brij-58
Vapor Induced phase separation
Non-solvent induced phase separation

ABSTRACT

This study investigates the modification of polyethersulfone (PES) membranes using the Brij-58 additive to enhance the hydrophilicity and antifouling performance of the resulting thin film for the separation of water pollutants. A combination of vapor-Induced phase separation (VIPS) and non-solvent induced phase separation (NIPS) methods was employed to ensure the retention of Brij-58 within the membrane matrix. SEM analysis revealed uniform pore distribution and symmetrical structure, while FTIR confirmed successful incorporation of Brij-58. The modified membrane (PB-90) exhibited improved hydrophilicity, as indicated by a reduced water contact angle from 75.31° to 55.11°. PB-90 also demonstrated the highest pure water flux (69.86 ± 1.294 L/m^2·h), though with a slight decrease in mechanical strength. Performance testing showed that PB-90 had superior antifouling characteristics, with a flux recovery ratio (FRR) of 91.91% and total fouling ratio (R_t) of 52.49%, compared to the unmodified membrane (PM) with an FRR of 75.70% and R_t of 25.58%. When applied to river water filtration, PB-90 significantly reduced contaminants. These results confirm that the incorporation of Brij-58 and the VNIPS technique effectively enhance the hydrophilic and antifouling properties of PES membranes.

* Corresponding author: Nasrul Arahman
E-mail: nasrular@usk.ac.id

GRAPHICAL ABSTRACT

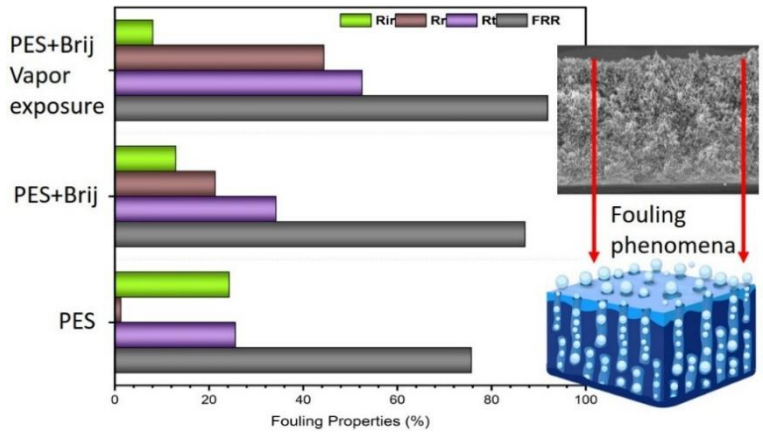

Introduction

Membrane technology has been widely used as an alternative in separation processes, such as water treatment [1], wastewater treatment [2], oil emulsion separation [3], hydrogen gas separation [4], desalination [5], and others. The use of technology continues to grow because membranes have various advantages, including relatively low energy use, high selectivity, and fairly easy operation [6]. In the water treatment process, membranes are used to remove various contaminants, such as particles or colloids [7], turbidity [8], organic substances [9], and bacteria [10].

In various membrane technology applications, the selection of membrane material plays a crucial role in determining process performance. PES is one of the most widely used polymers due to its excellent chemical resistance, mechanical strength, and thermal stability. However, PES is inherently hydrophobic, which makes it susceptible to fouling caused by the accumulation of organic and inorganic foulants on the membrane surface [11]. This fouling tendency can significantly impair membrane performance by reducing water flux, deteriorating permeate quality, and increasing energy consumption. Moreover, frequent cleaning and maintenance are required to mitigate fouling effects, thereby elevating operational costs and shortening membrane lifespan [12].

To address these limitations, various surface modification strategies have been developed to improve PES membrane hydrophilicity and antifouling performance. One of the most effective and practical methods is the incorporation of hydrophilic additives into the casting solution via the NIPS technique. This strategy enhances membrane wettability, improves fouling resistance, and allows for better control over pore structure and morphology [13,14].

Numerous studies have reported the successful modification of PES membranes using different hydrophilic additives. For instance, polyethylene glycol (PEG) has been widely used to improve water flux and hydrophilicity due to its strong affinity for water [15]. Polyvinylpyrrolidone (PVP) is another common additive that improves porosity and reduces fouling [16]. Graphene oxide (GO), a hydrophilic nanomaterial, has been shown to enhance both permeability and antifouling properties when blended with PES [17]. Cellulose nanocrystals (CNC) have also been incorporated to introduce hydroxyl groups and improve membrane surface hydrophilicity [18]. Additionally, the use of Pluronic F127, a block copolymer surfactant, has been demonstrated to significantly improve antifouling characteristics and overall membrane performance [19].

For example, [20] developed PES membranes incorporating PEGHE and nanocarbon additives, achieving a water flux of 63.17 L/m^2.h and Mg^{2+} rejection of 96.45%. Similarly, [21] demonstrated that the addition of Brij-58, a non-ionic surfactant, positively influenced membrane morphology and performance. These findings underscore the significance of additive-assisted membrane modification in optimizing PES membrane functionality.

Meanwhile, the incorporation of hydrophilic additives using the VIPS technique has also been introduced as a promising strategy to enhance the hydrophilic properties of PES membranes. Unlike the conventional NIPS method, VIPS allows for more controlled phase inversion by exposing the cast film to humid air before immersion in a coagulation bath. This slower demixing process facilitates the retention of hydrophilic additives, resulting in a more hydrophilic membrane surface and improved performance.

Several studies have demonstrated the effectiveness of the VIPS method in enhancing the hydrophilicity and performance of PES membranes. The Saufi research group prepared PES membranes modified with GO via VIPS and observed increased water flux and a significant reduction in water contact angle, indicating improved hydrophilicity and antifouling properties [22,23] employed Pluronic F127, a triblock copolymer, as a hydrophilic additive in polysulfone (PSf) membranes and reported superior surface wettability and higher protein rejection compared to membranes fabricated using the conventional NIPS method. [24] incorporated PEG into polyvinylidene fluoride (PVDF) membrane and found enhanced surface hydrophilicity, and resistance to fouling. Similarly, [25] reported that incorporating Pluronic F127 into PES membranes using VIPS significantly enhanced water flux, reduced fouling tendencies, and improved surface hydrophilicity compared to the unmodified counterparts.

In summary, membrane surface properties and morphological structures can be effectively tailored through the incorporation of hydrophilic additives using either the NIPS or VIPS techniques. Both approaches have been shown to enhance membrane performance, particularly in terms of permeability and fouling resistance, when compared to unmodified membranes.

In the present study, a more advanced fabrication strategy is employed by integrating both NIPS and VIPS methods referred to as vapor and VNIPS to develop PES membranes with superior hydrophilicity and filtration performance. Brij-58 was employed as a hydrophilic additive to enhance the surface properties of the PES membrane. The membrane was fabricated using the Vapor and VNIPS technique, which is expected to yield membranes with optimized structural and performance characteristics. In this process, the cast membrane film is first exposed to air at controlled humidity levels before immersion in a non-solvent coagulation bath. This intermediate exposure step facilitates the partial evaporation of solvent and allows for the entrapment of hydrophilic additives within the polymer matrix, thereby enhancing membrane functionality.

Experimental

Materials

PES (Ultrason E6020P) was used as the polymer and dimethylacetamide (Wako Pure Chemical Industries, Japan) was used as the solvent. Brij-58 (Sigma Aldrich Co., LLC, Germany, Mw 1,124) was added as an additive. Humic acid (Sigma Aldrich Co., LLC, Germany) was used as an organic contaminant. Distilled water was used as the non-solvent during membrane solidification.

Membrane Preparation

The membrane fabrication process involved the preparation of three different dope solutions. The first solution, designated as PM, was prepared by dissolving 16 wt% PES in *N,N*-dimethylacetamide (DMAc) as the solvent. The second formulation, labeled PB, consisted of 16 wt% PES and 3 wt% Brij-58, a non-ionic surfactant, dissolved in DMAc. Both solutions were magnetically stirred for 24 hours at ambient temperature to ensure complete dissolution and homogeneity, followed by degassing for 15 minutes to remove entrapped air bubbles. The casting process was performed on a clean glass plate using a casting knife set to a wet film thickness of 300 μm. Phase inversion was subsequently induced by immersing the cast film into a non-solvent coagulation bath (typically deionized water). For the third membrane, referred to as PB-90, the same composition as PB (16 wt% PES and 3 wt% Brij-58 in DMAc) was utilized. However, the fabrication process incorporated a vapor exposure step characteristic of the VNIPS technique. Specifically, following

casting, the membrane film was exposed to a humid atmosphere with 90% relative humidity for 15 seconds to initiate controlled phase separation before being immersed in the non-solvent coagulation bath. This intermediate exposure allows for partial solvent evaporation and regulated demixing, which promotes more effective integration of the hydrophilic additive into the polymer matrix and facilitates the development of a more uniform, defect-free, and structurally optimized membrane. A schematic representation of the membrane preparation procedure is displayed in Figure 1.

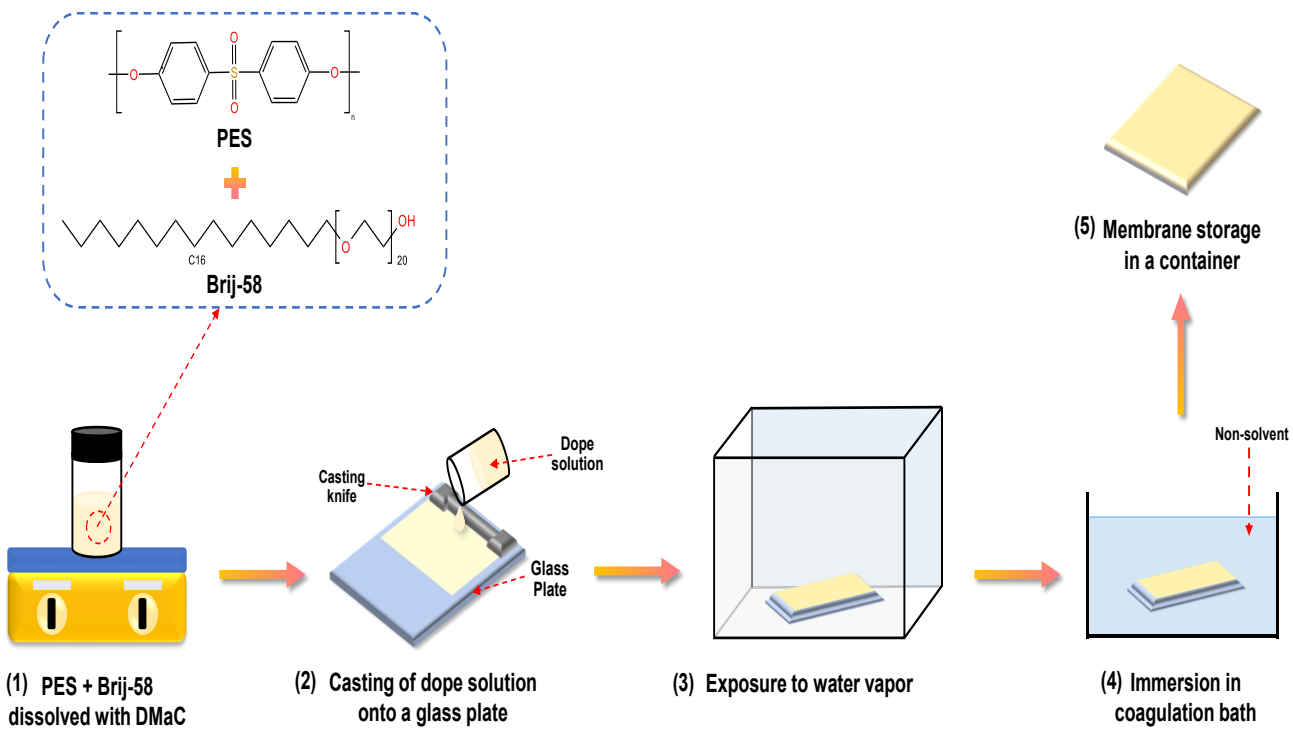

Figure 1: Membrane preparation procedure

Membrane Characterization

The surface and cross-sectional morphologies of the membranes were examined using a field-emission scanning electron microscope (FESEM; JSF-7500F; JEOL, Ltd., Tokyo, Japan). Prior to imaging, membrane samples were fractured in liquid nitrogen to preserve the internal structure, followed by sputter-coating with a thin layer of gold to enhance conductivity and image resolution. SEM micrographs were captured at 6,000 magnifications to observe pore distribution, skin layer thickness, and internal porous structures.

The chemical composition and functional groups present on the membrane surface were characterized using fourier transform infrared (FTIR) spectroscopy (Nicolet iS5, Thermo Scientific, USA). The analysis was carried out in the range of 4000–400 cm^{-1} using the attenuated total reflectance (ATR) mode. This technique allowed the identification of characteristic absorption bands associated with specific chemical bonds and functional group modifications after membrane fabrication or surface treatment.

Membrane surface hydrophilicity was evaluated by measuring the static water contact angle using a contact angle goniometer (Drop Master DM-300, Kyowa Interface Science Co., Saitama, Japan). A droplet of deionized water (5 µL) was carefully placed on the membrane surface, and the contact angle was recorded after 5 seconds using an integrated camera system and software. Each measurement was repeated at ten different points on the membrane surface, and the average value was reported to ensure accuracy and reproducibility.

The mechanical properties of the membranes were assessed using a universal testing machine in accordance with ASTM D638-14 standard. Membrane samples were cut into dumbbell-shaped specimens and conditioned at room temperature before testing. The tensile strength was measured using a constant rate of elongation until failure. This analysis provided insights into the durability and suitability of the membrane for pressure-driven separation applications.

Membrane Filtration Test

The membrane performance was evaluated using a crossflow filtration module operated at 0.1 MPa. A peristaltic pump maintained a continuous feed flow, while valves regulated the operating pressure, monitored by a manometer. The schematic diagram of the setup is presented in Figure 2. Membrane samples were cut to fit the module and compacted to achieve structural stability and a steady pure water flux for 1 h. Following compaction, the permeation test was conducted by collecting and weighing permeate at 10 minutes intervals until a steady-state flux was reached. The pure water flux was determined using Equation 1 [26].

$$J = \frac{V_p}{A \times \Delta t} \quad (1)$$

Where, J is the pure water flux (L/m².h), V_p is the permeate volume produced every 10 minutes (L), A is the membrane area used (m²), and Δt is the test time (h).

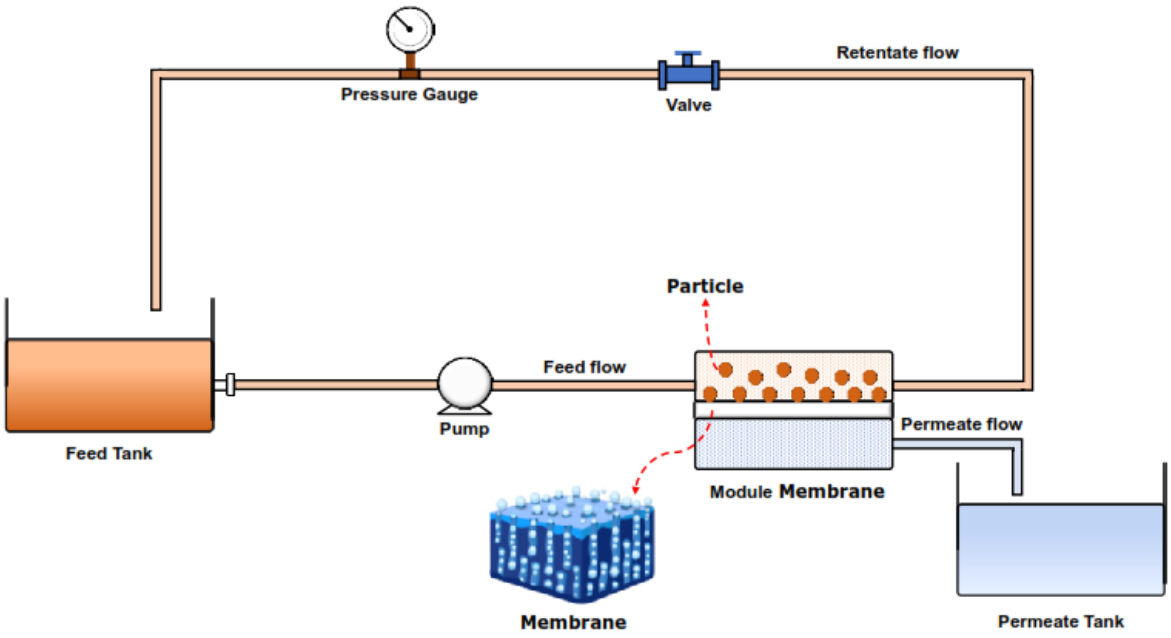

Figure 2: Schematic of crossflow filtration system

Antifouling Properties Test

The antifouling performance of the membrane was evaluated by assessing its resistance to organic foulants during filtration. The test employed the same setup as the pure water flux measurement but was conducted in three sequential stages. First, the membrane underwent pure water filtration for 60 minutes to establish baseline permeability. In the second stage, a 50 mg/L humic acid solution was used as a model foulant, and the membrane was subjected to humic acid filtration under identical conditions. After fouling, the membrane was cleaned via reverse flushing for 10 minutes. In the final stage, the membrane was tested again with pure water for 60 minutes to assess flux recovery.

The antifouling performance of the membrane is analyzed using the ratio of pure water flux comparison after pollutant filtration to pure water flux, namely FRR, which can be calculated using Equation 2. The amount of fouling that can be removed by the membrane washing process is called reversible fouling (R_r), calculated using

Equation 3. In addition, the accumulation of fouling that remains on the membrane after washing is called irreversible fouling (Rir) which can be calculated using Equation 4. The total of fouling that can be removed and remains on the membrane is called the total fouling ratio (R_t) which is calculated using Equation 5 [27,28].

$$FRR = \left(\frac{J_R}{J_0}\right) \times 100\% \quad (2)$$

$$R_r = \left(\frac{J_R - J_p}{J_0}\right) \times 100\% \quad (3)$$

$$R_{ir} = \left(\frac{J_0 - J_R}{J_0}\right) \times 100\% \quad (4)$$

$$R_t = \left(1 - \frac{J_p}{J_0}\right) \times 100\% \quad (5)$$

Where, J_0 is the flux of pure water (L/m².h), J_p is the flux of the water sample containing pollutants (L/m².h), and J_R is the flux of pure water after pollutant filtration (L/m².h).

Filtration Application to River Water

Membrane was applied for the separation of contaminants in Lamnyong River water in Banda Aceh. Samples were first treated by precipitating suspended solids. Furthermore, the sample was carried out with a crossflow type filtration device. The permeate obtained was tested for analysis of water quality parameters including turbidity, total suspended solid (TSS), *E. coli* bacteria, and coliform. The rejection efficiency was calculated using Equation 6 [29].

$$Rm = \left(1 - \frac{C_p}{C_f}\right) \times 100\% \quad (6)$$

Where, R_m is the rejection value (%), C_p is the permeate concentration (mg/L), and C_f is the feed concentration (mg/L).

Results and Discussion

Membrane Characteristics

The SEM images of the membrane surface and cross-section under different fabrication conditions are presented in Figure 3. The PM membrane, fabricated via the NIPS method without air exposure, exhibited a typical asymmetric structure comprising a dense skin layer, a thick supporting layer, and a substructure dominated by finger-like macrovoids with minor sponge-like regions. In contrast, the PB membrane, modified with 3 wt% Brij-58, displayed a higher surface pore density and increased formation of finger-like macrovoids. This behavior is attributed to the amphiphilic nature of Brij-58, which promotes faster water ingress during phase inversion by enhancing solvent–non-solvent exchange [20]. Meanwhile, the PB-90 membrane, fabricated via the VNIPS technique with 15 seconds of exposure to 90% relative humidity prior to immersion, exhibited a more homogeneous and symmetric morphology with a sponge-like porous substructure and dense surface pore distribution. The absence of macrovoids in this membrane is likely due to the partial diffusion of water vapor during air exposure, which moderates the demixing rate and suppresses macrovoid formation during coagulation [30]. Similar findings were reported by [31], who observed sponge-like structures without macrovoids in PSF membranes fabricated under humid air exposure, highlighting the role of vapor-induced phase control.

The functional groups on the membrane were analyzed using FTIR spectroscopy. Figure 4 shows the FTIR spectra of the PES membrane before and after modification. The PM membrane shows asymmetric stretching of –SO_2– group (1,148 cm^{-1}), bending vibration of O=S=O group (554 cm^{-1}), stretching vibration of C=C ring (1,484 cm^{-1}), and asymmetric stretching of C–O–C group (1238 cm^{-1}). In another study, it was also reported that similar functional groups were found in pure PES membranes [8]. PB and PB-90 membranes

modified with Brij-58 showed some differences in FTIR spectra compared to PM membranes, namely the appearance of stretching vibration of hydrophilic group $–CH_2–O–CH_2–$ (948–951 cm^{-1}) and asymmetric stretching of hydrophobic group $–CH_2–CH_3$ (2,856–2,930 cm^{-1}) [22]. These results indicate that the membrane modification with Brij-58 is able to maintain the presence of additives on the membrane surface during the immersion process in the coagulation bath.

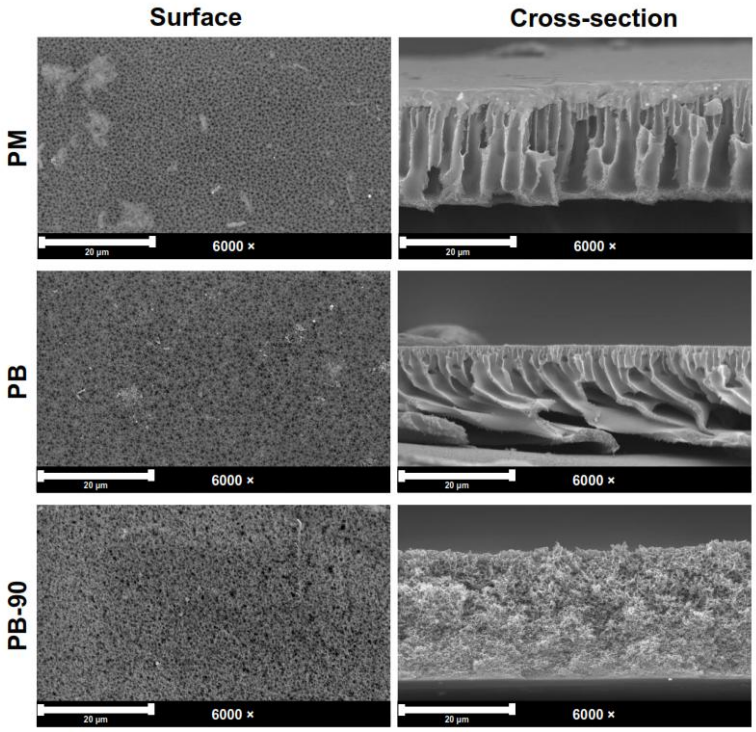

Figure 3: SEM test results of membrane surface and cross-section

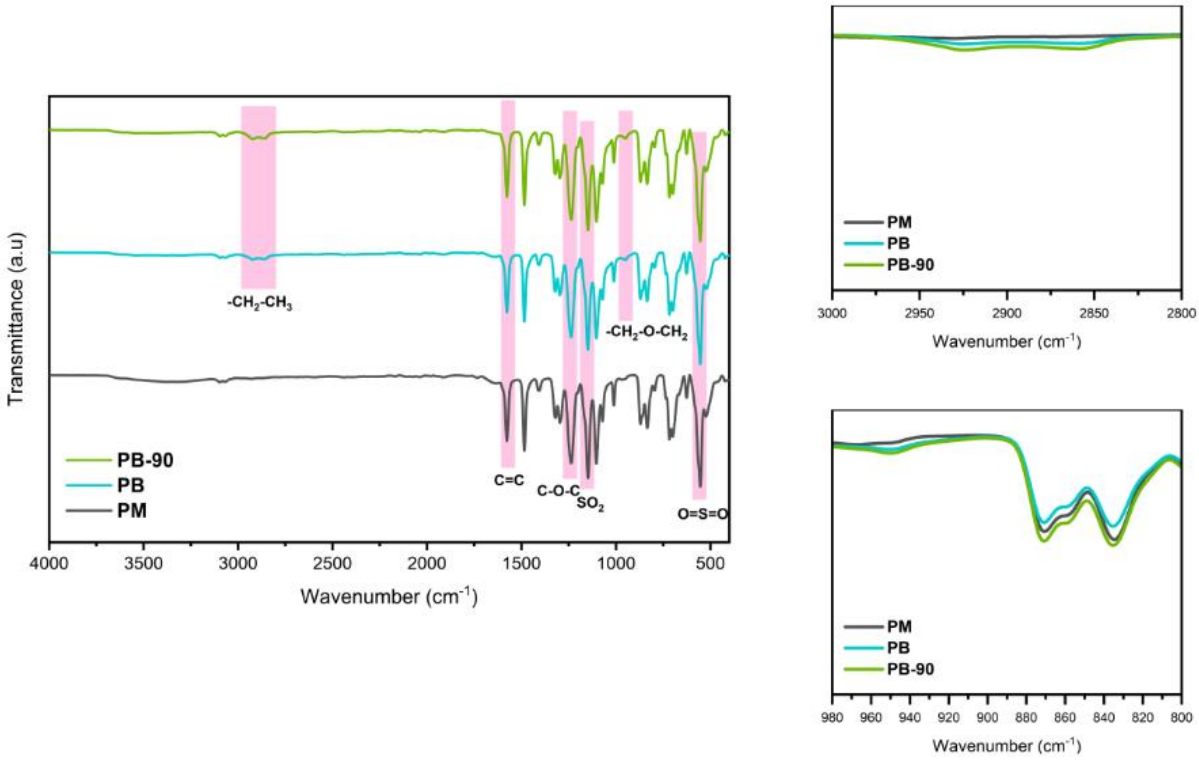

Figure 4: FTIR spectrum

The hydrophilicity of the membrane surface measured through the water contact angle showed a decrease from the NIPS membrane to the VNIPS membrane (Table 1). The PM membrane had a WCA of 75.31° + 0.5. When Brij-58 was added, the contact angle decreased to 60.05° + 3.224. The addition of additives was shown to increase the hydrophilicity of the membrane, which was characterized by a decrease in the water contact angle value. This hydrophilic nature also affects the formation of membrane pores, as it increases the interaction with water thus accelerating the diffusion between solvent and non-solvent in the coagulation bath [19]. Meanwhile, the membrane made with VNIPS showed a further decrease in water contact angle, which became 55.11° + 0.398. This decrease is due to the increasing amount of hydrophilic poly(ethylene oxide) (PEO) chains contained in the structure of Brij-58 on the membrane surface. The PEO segments promote strong interactions with water molecules through hydrogen bonding, forming a hydration layer that enhances surface wettability and reduces the WCA. In another study, [29] reported that the incorporation of non-ionic surfactant additives such as Poloxamer 188, which contain PEO chains, can enhance membrane hydrophilicity [24]. also reported a decrease in the water contact angle of PES-kaolin membranes prepared by the VNIPS method. By providing exposure to air, the water contact angle decreased from 73.80° + 3.66 to 67.26 + 2.45.

In describing the mechanical properties of a membrane, tensile strength is the main parameter. To avoid damage to the membrane structure during the filtration process, it is necessary to measure its tensile strength and flexibility. Generally, membranes with a denser structure have better breaking strength compared to porous membrane [32]. The results of the tensile strength test are shown in Table 1. The PM membrane shows the highest tensile strength value of 1.08 kgf/mm^2. However, the tensile strength of the PB membrane decreased to 0.89 kgf/mm^2. Furthermore, the PB-90 membrane prepared by VNIPS method shows a further reduction to 0.82 kgf/mm^2. This reduction can be attributed to the plasticizing effect of the surfactant and the development of microstructural defects due to phase separation, which increase polymer chain mobility and free volume, thereby lowering the tensile strength of the membrane [33].

Table 1 also shows the effect of air exposure on membrane flux values. PM membrane has the lowest flux value, which is 25.53 + 3.005 L/m^2.h. The membrane flux value (PB) increased to 36.97 + 3.13 L/m^2.h after the membrane was added with Brij-58 additive. [21] reported that PES membrane modified with Brij-58 additive obtained flux value of 7.84 - 52.1 L/m^2.h.bar. In addition, the membrane exposed to air showed a significant increase in flux of 69.86 + 1.294 L/m^2.h. This is due to the very strong interaction with air, as well as the very strong interaction between the membrane surface and water molecules, so that water passes through the membrane more easily [34].

Table 1: Membrane characteristics

Membrane code	WCA (°)	Tensile strength (kgf/mm^2)	Flux (L/m^2.h)
PM	75.31 + 0.5	1.08	25.53 + 3.005
PB	60.05 + 3.224	0.89	36.97 + 3.13
PB-90	55.11 + 0.398	0.82	69.86 + 1.294

Antifouling Performance

Figure 5a illustrates the water flux profiles of the membranes as a function time during the antifouling tests. In the initial filtration stage (0-60 minutes), the flux of all membranes was relatively stable, with the PB-90 membrane showing the highest flux value compared to the PB and PM membranes. In the second stage (60-120 minutes), a decline in flux was observed for all membranes due to the formation of fouling layers on the membrane surface and within the membrane pores, which hindered permeate flow. After the membrane washing process (120-180

minutes the flux increased again for all membranes, with the highest flux recovery observed for the PB-90 membrane. This behaviour can be attributed to the presence of a hydrated layer and a more uniform pore distribution in the PB-90 membrane, which facilitates more effective removal of foulants from the membrane surface [35].

The fouling properties analysis (Figure 5b) revealed significant differences among the membranes in terms of R_t, reversible fouling (R_r), irreversible fouling (R_{ir}), and FRR. Overall, the results indicate that membranes modified with Brij-58 and air exposure improved antifouling performance compared to the pristine PES membrane. The PM membrane have the lowest FRR value of 75.70% with a total flux loss of 25.58% improved antifouling performance compared to the pristine PES membrane. Meanwhile, the PB-90 membrane exhibited the highest FRR value of 91.91%, indicating excellent flux recovery after membrane cleaning. Nevertheless, the PB-90 membrane showed a higher total flux loss than the PM membrane, reaching 52.49%. This behaviour can be attributed to the more uniform pore distribution on the membrane surface, which facilitates the adhesion of humic acid during filtration. However, the reversible fouling of the PB-90 membrane increased to 44.40%, indicating that a large fraction of the fouling was reversible. This result suggests improved fouling resistance, as also reported by [36]. In addition, the relatively low irreversible fouling of the PB-90 membrane (8.09%) indicates enhanced membrane cleanability, which is favourable for maintaining membrane performance during long-term operation.

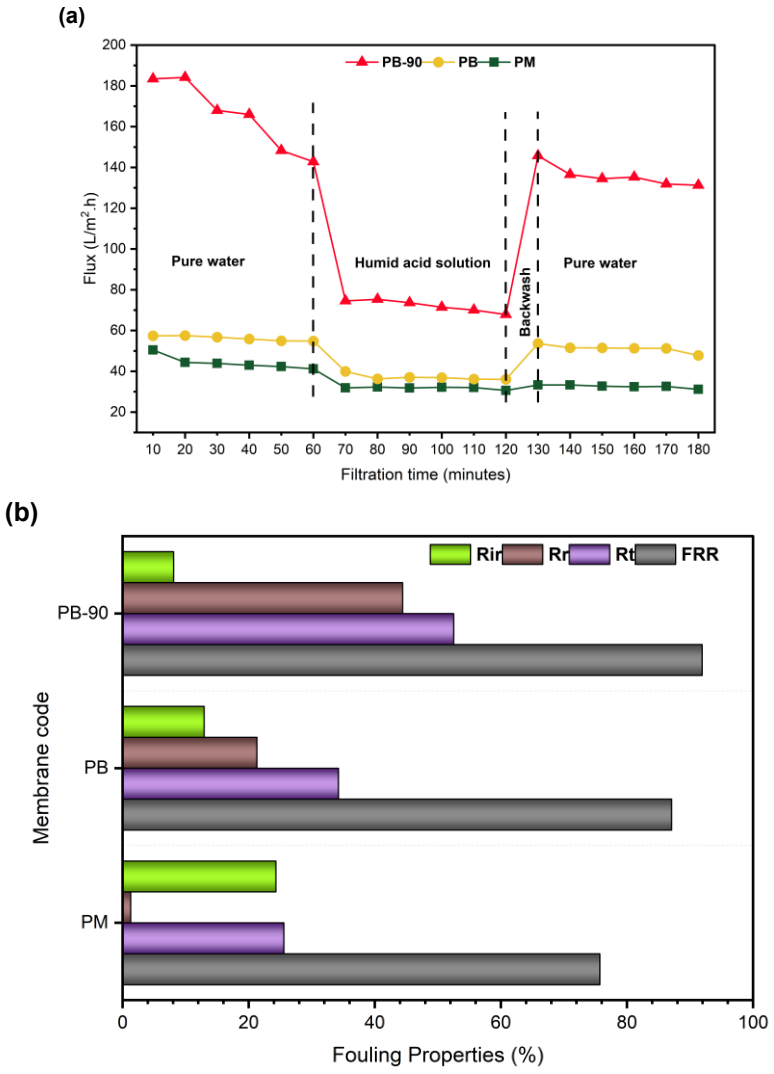

Figure 5: Evaluation of membrane performance (a) membrane flux vs filtration time and (b) membrane fouling properties

Water Turbidity

Figure 6 shows the filtration results of the river water turbidity test. The initial water turbidity of 16.33 NTU was reduced to 0.72 NTU after filtration using the membrane. The PM membrane is able to reduce the turbidity of river water by 89.16%, while the modified membrane has a significant increase in rejection up to 95.59% which shows that the membrane is able to retain the particles in the river water well. The findings show that PB-90 membrane modified by VNIPS method has an advantage in reducing turbidity. The turbidity value of water after filtration using the membrane has met the allowable turbidity value [37]. Another study, [38], conducted river water filtration with activated carbon discs modified by PES membrane using activated carbon. The results showed that the membrane was able to reduce turbidity by 79%.

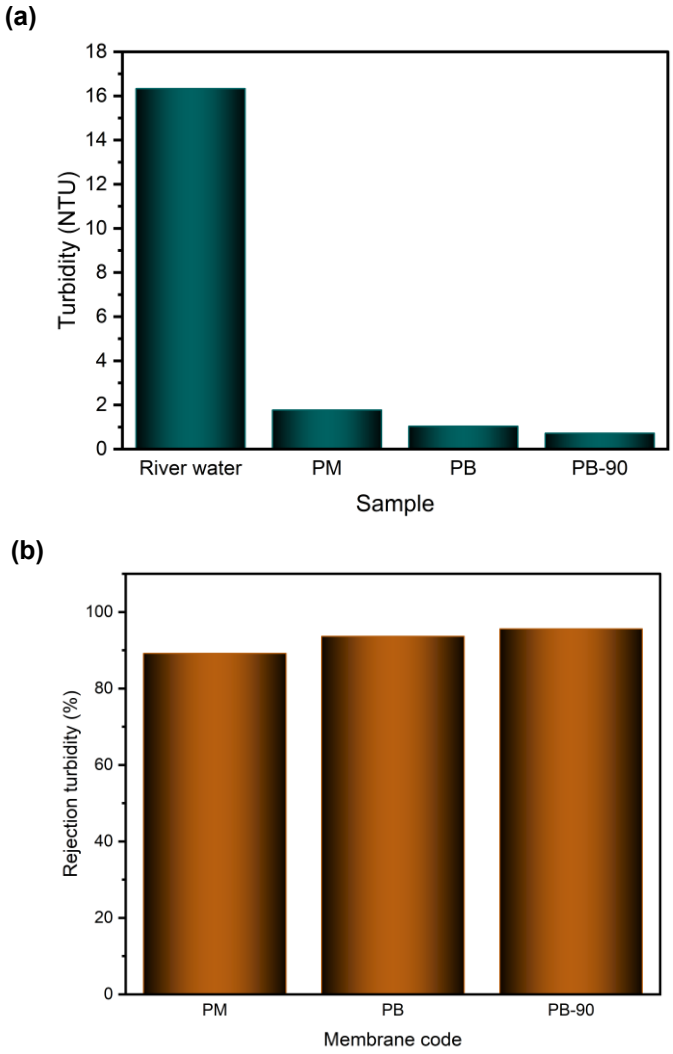

Figure 6: (a) River water turbidity test results and (b) river water turbidity rejection

TSS

Figure 7a presents the TSS results before and after filtration using PM, PB, and PB-90 membranes. The initial TSS concentration of 231.5 mg/L decreased to 2 mg/L after membrane filtration, indicating the high effectiveness of the membranes in removing TSS from river water. However, TSS reduction alone is insufficient to classify the treated water as drinking water, since comprehensive evaluation of additional physicochemical and microbiological parameters is required in accordance with established drinking water quality standards. Therefore, the filtered water is more appropriately classified as clean water with potential for further treatment.

Figure 7b shows the TSS rejection values by PM, PB, and PB-90 membranes. PB membrane has the highest TSS rejection performance at 99.14%, followed by PM and PB-90 membranes at 98.70 and 98.27%. The membrane rejection results showed very good numbers, but there was a decrease in rejection on the PB-90 membrane. This is due to the pore distribution on the membrane allowing TTS to pass during the filtration process. The research by [39] Al-Tamimi have conducted filtration of Tigris river water in Baghdad using ultrafiltration membranes showing a TSS value of 88%.

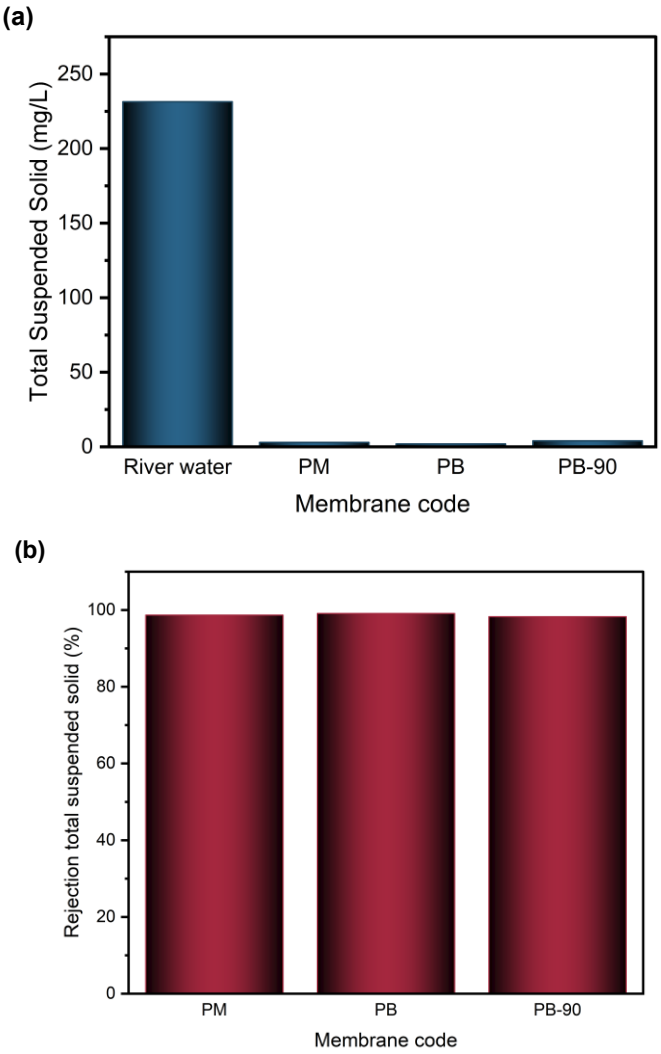

Figure 7: (a) TSS before and after filtration and (b) rejection of TSS

Total Coliform and E.coli Counts

Figure 8 show the results of total coliform and *E. coli* analysis before and after filtration. Initially, the coliform content in the river water was 93 MPN/mL, while the *E. coli* count reached 3 MPN/mL. After going through the filtration process using membranes, there was a significant decrease in the content of microorganisms. These results indicate that filtration using membranes can effectively reduce the amount of coliform and *E. coli* in water. These findings also indicate that modification of the membrane with Brij-58 contributes to the antibacterial properties of the membrane. Tshangana has also reported that using pes membranes modified with graphene quantum dots (GQDs) can reduce bacterial growth which supports the potential of material modification in improving the antimicrobial performance of membranes [40].

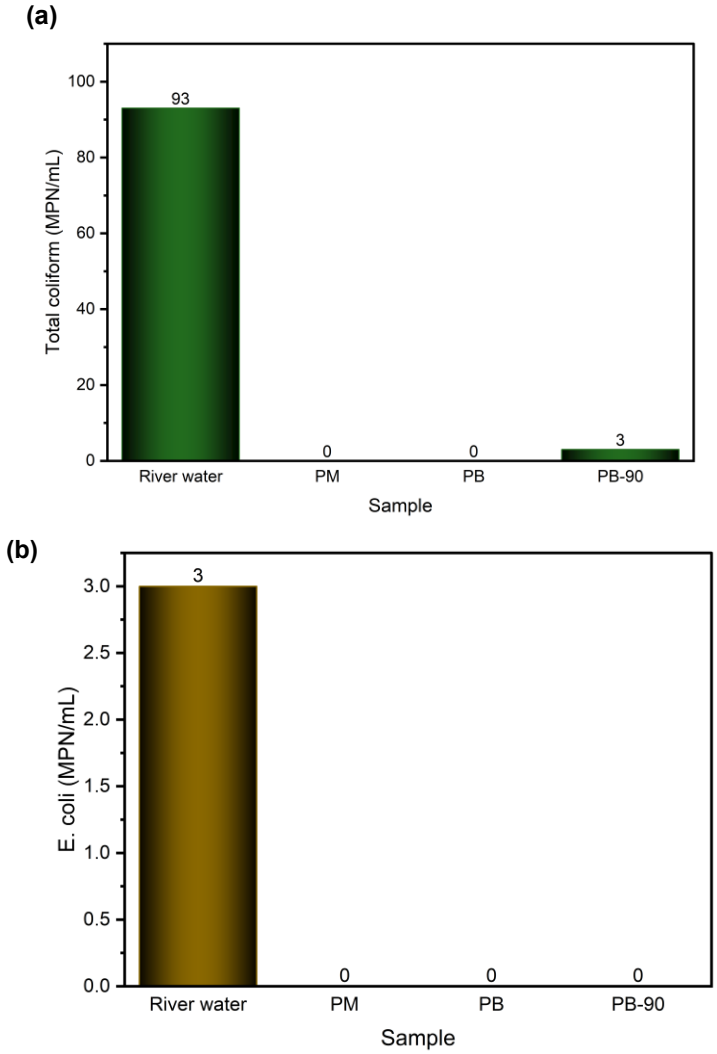

Figure 8: (a) Total coliform and (b) *E. coli* before and after filtration

Conclusions

Modification of PES membrane by VNIPS method and addition of Brij-58 effectively improved the hydrophilic properties as well as antifouling ability of the membrane. Membrane characterization showed significant changes in surface morphology and pore distribution. The results of filtration application to river water showed that the membrane can reduce various water quality parameters, such as turbidity, TSS, and microorganism activity. This decrease indicates that the filtration performance of the membrane is excellent. These findings strengthen the potential of Brij-58 modified PES membrane using VNIPS method as an alternative in water treatment.

Conflict of Interest

The author declared no conflict of interest

Consent for Publications

All authors declared that they read and approved the final version of the manuscript for publication.

Availability of Data and Material

Not applicable.

Authors' Contributions

Miftahul Arzaq: Writing - original draft and data curation. Muhammad Az-Harry: Writing draft, methodology, and data analysis. Haziqia Aulia Putri and Nasywa Humaira Nasrul: Researching data processing. Sri Mulyati: Writing – review &

editing. Cut Meurah Rosnelly: Writing – review & editing. Muhammad Proyogie Aulia: Writing – review & editing. Nafiu Umar Barambu: Writing – review & editing. Nasrul Arahman: Writing – review & editing, supervision, and conceptualization.

Acknowledgement

The authors would like to acknowledge Universitas Syiah Kuala for the financial support of this work through the PDRA research grant (487/UN11/SPK/PNBP/2024). They would also like to gratefully acknowledge the Indonesian Endowment Fund for Education (LPDP), under the Ministry of Higher Education, Science and Technology, through the EQUITY Program (Contract No. 4318/B3/DT.03.08/2025 and No. 491/UN11/HK.02.06/2025), for supporting the article processing charge (APC) of this publication.

ORCID

Miftahul Arzaq
https://orcid.org/0009-0007-5668-7373
Muhammad Az-Harry
https://orcid.org/0009-0006-1742-379X
Haziqia Aulia Putri
https://orcid.org/0009-0000-5959-6716
Nasywa Humaira Nasrul
https://orcid.org/0009-0000-9563-2032
Sri Mulyati
https://orcid.org/0000-0001-5865-4769
Cut Meurah Rosnelly
https://orcid.org/0000-0003-0531-3674
Nafiu Umar Barambu
https://orcid.org/0000-0001-5641-1317
Muhammad Prayogie Aulia
https://orcid.org/0000-0001-6389-7810
Nasrul Arahman
https://orcid.org/0000-0001-5077-2867

References

[1] Li, M., Huang, G., Chen, X., Xiao, H., An, C., Yin, J., Xin, X. Development of an antimicrobial and antifouling PES membrane with ZnO/poly(hexamethylene biguanide) nanocomposites incorporation. *Chemical Engineering Journal*, **2024**, 481, 148744.
[2] Mulyati, S., Muchtar, S., Yusuf, M., Arahman, N., Sofyana, S., Rosnelly, C.M., Shamsuddin, N. Production of high flux poly(ether sulfone) membrane using silica additive extracted from natural resource. *Membranes*, **2020**, 10(1), 17.
[3] Aulia, M.P., Gonzales, R.R., Tabuchi, M., Kitagawa, T., Okamoto, Y., Zhang, P., Matsuyama, H. Chitin-augmented wetting resistance and water-in-oil emulsion separation performance of silane-modified polyketone membrane. *Journal of Membrane Science*, **2024**, 710(123115.
[4] Marsico, L., Brunetti, A., Catizzone, E., Migliori, M., Barbieri, G. Integrated membrane gas separation process for the valorisation of H_2 and CO_2 to biomethane. *Renewable Energy*, **2025**, 123693.
[5] Yang, J., Yu, C., Hinkle, K.R., Gu, Z. Porous boron carbide (BC_3) membranes for highly efficient seawater desalination: the critical role of fine-tuning shape and composition in BC_3 nanopores. *Desalination*, **2025**, 119063.
[6] Motloutsi, M.L., Matebese, F., Madito, M.J., Motsa, M.M., Managa, M., Moutloali, R.M. Zwitterion functionalized graphene oxide thin film nanocomposite membrane for brackish water desalination and natural organic matter removal. *Desalination and Water Treatment*, **2025**, 323, 101276.
[7] Guo, D., Xu, J., Zhang, X., Wong, N.H., Sunarso, J., Liu, S., Li, N. Fabrication of knitted Polyethylene/SiO_2 composite membrane modules for one-step microfiltration and particle removal in wastewater treatment. *Composites Science and Technology*, **2024**, 250, 110479.
[8] Al-Furaiji, M.H., Kalash, K.R., Kadhom, M.A., Alsalhy, Q.F. Evaluation of polyethersulfone microfiltration membranes embedded with MCM-41 and SBA-15 particles for turbidity removal. *Desalination and Water Treatment*, **2021**, 215, 50-59.
[9] Paziresh, S., Dehqan, A., Zinadini, S., Zinatizadeh, A.A., Vatanpour, V. Rosemary particle as a new green additive to improve polysulfone membrane separation performance in removal of organic pollutants. *Separation and Purification Technology*, **2024**, 334, 126015.
[10] Ishak, N.I.I., Boon Seng, O., Juinn Chieh, D.C., Koe Zhen Yao, A., Ying Shi, C., Qi Hwa, N. Treatment of river water using modular gravity-driven ultrafiltration (GDU) for individual contingency water supply. *Water Supply*, **2022**, 22(5), 5618-5637.
[11] Wen, X., He, C., Hai, Y., Ma, R., Sun, J., Yang, X., Chen, J. Fabrication of an antifouling PES ultrafiltration membrane via blending SPSF. *RSC Advances*, **2022**, 12(3), 1460-1470.
[12] Huang, C., Huang, P., Yang, W., Liu, J., Zeng, H. Co-hydrolyzed bio-inspired antifouling coatings for functional membranes in oily wastewater treatment. *Journal of Colloid and Interface Science*, **2025**, 138197.
[13] Alanezi, A.A., Abdallah, H., Shalaby, M.S., Aljumaily, M.M., Alsalhy, Q.F., Shaban, M., Hernadi, K. Super-antifouling PES nanocomposite membrane encapsulated silica nanoparticles and coated nano-Ag/polyvinyl alcohol layer. *Alexandria Engineering Journal*, **2024**, 91, 103-114.
[14] Otitoju, T.A., Ahmad, A.L., Ooi, B.S. Recent advances in hydrophilic modification and performance of

polyethersulfone (PES) membrane via additive blending. *RSC Advances*, **2018**, 8(40), 22710-22728.
[15] Adeniyi, A., Odo, G.O., Gonzalez-Ortiz, D., Pochat-Bohatier, C., Mbakop, S., Onyango, M.S. A comparison of the effect of cellulose nanocrystals (CNCs) and polyethylene glycol (PEG) as additives in ultrafiltration membranes (PES-UF): Characterization and performance. *Polymers*, **2023**, 15(12), 2636.
[16] Acarer, S. Effect of different solvents, pore-forming agent and solubility parameter differences on the properties of PES ultrafiltration membrane. *Sakarya University Journal of Science*, **2022**, 26(6), 1196-1208.
[17] Adnan Maykhan, N., Alsalhy, Q.F., Bakhtiari, O. Incorporation of graphene oxide nanosheets into polyethersulfone membranes to improve their separation performance and antifouling characteristics for Congo red removal. *Water Environment Research*, **2023**, 95(5), e10866.
[18] Zhang, D., Karkooti, A., Liu, L., Sadrzadeh, M., Thundat, T., Liu, Y., Narain, R. Fabrication of antifouling and antibacterial polyethersulfone (PES)/cellulose nanocrystals (CNC) nanocomposite membranes. *Journal of Membrane Science*, **2018**, 549, 350-356.
[19] Teli, S.B., Benamor, A., Nasser, M., Hawari, A., Zaidi, S.J., Ba-abbad, M., Mohammad, A.W. Effects of amphiphilic pluronic F127 on the performance of PS/SPEEK blend ultrafiltration membrane: Characterization and antifouling study. *Journal of Water Process Engineering*, **2017**, 18, 176-184.
[20] Haikal, R., Marom, A., Aulia, M., Ambarita, A., Azwar, A., Fahrina, A., Koyuncu, İ. Morphology and characteristics of polyethersulfone membrane modified with polyethylene glycol hexadecyl ether and nanocarbon. *Applied Chemical Engineering*, **2023**, 7(1).
[21] Mulyati, S., Arahman, N., March. Influence of Brij58 on the characteristic and performance of pes membrane for water treatment process. In *IOP Conference Series: Materials Science and Engineering*. 2017, 180, 012130.
[22] Harruddin, N., Saufi, S.M., Faizal, C.K.M., Mohammad, A.W. Effect of VIPS fabrication parameters on the removal of acetic acid by supported liquid membrane using a PES–graphene membrane support. *RSC Advances*, **2018**, 8(45), 25396-25408.
[23] Plisko, T., Penkova, A., Burts, K., Bildyukevich, A., Dmitrenko, M., Melnikova, G., Missyul, A. Effect of Pluronic F127 on porous and dense membrane structure formation via non-solvent induced and evaporation induced phase separation. *Journal of Membrane Science*, **2019**, 580, 336-349.
[24] Mat Nawi, N.I., Chean, H.M., Shamsuddin, N., Bilad, M.R., Narkkun, T., Faungnawakij, K., Khan, A.L. Development of hydrophilic PVDF membrane using vapour induced phase separation method for produced water treatment. *Membranes*, **2020**, 10(6), 121.
[25] Xu, M.H., Xie, R., Ju, X.J., Wang, W., Liu, Z., Chu, L.Y. Antifouling membranes with bi-continuous porous structures and high fluxes prepared by vapor-induced phase separation. *Journal of Membrane Science*, **2020**, 611, 118256.
[26] Fathanah, U., Muchtar, S., Aprilia, S., Lubis, M.R., Mulyati, S., Yusuf, M. Unlocking synergies of $Mg(OH)_2$ and rice husk silica as dual additives for tailored pore properties, selectivity, and antifouling performances of PES membrane. *South African Journal of Chemical Engineering*, **2024**, 48(1), 22-29.
[27] Mulyati, S., Muchtar, S., Arahman, N., Meirisa, F., Syamsuddin, Y., Zuhra, Z., Wirzal, M.D.H. One-pot polymerization of dopamine as an additive to enhance permeability and antifouling properties of polyethersulfone membrane. *Polymers*, **2020**, 12(8), 1807.
[28] Muslim, A., Supardan, M.D., Ambarita, A.C., Arahman, N. Combination of cellulose nanocrystal and graphene oxide as modifying agent for improving the performance of PVDF membranes. *Case Studies in Chemical and Environmental Engineering*, **2024**, 10, 100873.
[29] Arahman, N., Rosnelly, C.M., Windana, D.S., Fahrina, A., Silmina, S., Maimun, T., Bilad, M.R. Antimicrobial hydrophilic membrane formed by incorporation of polymeric surfactant and patchouli oil. *Polymers*, **2021**, 13(22), 3872.
[30] Wang, X., Chen, D., He, T., Zhou, Y., Tian, L., Wang, Z., Cui, Z. Preparation of lateral flow pvdf membrane via combined vapor-and non-solvent-induced phase separation (V-NIPS). *Membranes*, **2023**, 13(1), 91.
[31] Ishak, N.I.I., Boon Seng, O., Juinn Chieh, D.C., Koe Zhen Yao, A., Ying Shi, C., Qi Hwa, N. Treatment of river water using modular gravity-driven ultrafiltration (GDU) for individual contingency water supply. *Water Supply*, **2022**, 22(5), 5618-5637.
[32] Arisandi, R., Fathurrahman, A., Fahrina, A., Razi, F., Jalil, Z., Arahman, N. Morphology and filtration performances of polyether sulfone membrane modified with carbon and Fe_2O_3. In *IOP Conference Series: Materials Science and Engineering*, **2020**, 845, 12018.
[33] Rastegar, B., Saljoughi, E., Mousavi, S.M., Kiani, S. Polyphenylsulfone/polyethylene glycol hexadecyl ether blend membranes with enhanced surface hydrophilicity for high-performance nanofiltration of dye solution. *Korean Journal of Chemical Engineering*, **2022**, 39(9), 2465-2473.
[34] Dehban, A., Kargari, A., Ashtiani, F.Z. Preparation and optimization of antifouling PPSU/PES/SiO_2 nanocomposite ultrafiltration membranes by VIPS-NIPS technique. *Journal of Industrial and Engineering Chemistry*, **2020**, 88, 292-311.
[35] Yu, X., Zhu, Y., Lu, Y., Wang, M., Huang, Z. Fabrication of dual ionic polymer nanofiltration membrane with deposited graphene oxide interlayer for enhanced flux and antifouling properties. *Desalination*, **2025**, 615, 119268.
[36] Barambu, N.U., Bilad, M.R., Bustam, M.A., Huda, N., Jaafar, J., Narkkun, T., Faungnawakij, K. Development of polysulfone membrane via vapor-induced phase separation for oil/water emulsion filtration. *Polymers*, **2020**, 12(11), 2519.
[37] Arahman, N., Jakfar, J., Dzulhijjah, W.A., Halimah, N., Silmina, S., Aulia, M.P., Bilad, M.R. Hydrophilic

antimicrobial polyethersulfone membrane for removal of turbidity of well-water. *Water*, **2022**, 14(22), 3769.
[38] Prihandana, G.S., Sururi, A., Sriani, T., Yusof, F., Jamaludin, M.F., Mahardika, M. Facile fabrication of low-cost activated carbon bonded polyethersulfone membrane for efficient bacteria and turbidity removal. *Water Practice & Technology*, **2022**, 17(1), 102-111.
[39] Al-Tamimi, N.J., Al-Alawy, A.F., Al-Shaeli, M. Evaluation of microfiltration and ultrafiltration membranes for improving water quality: Removal of turbidity, suspended solids, and bacteria from the Tigris River. *Iraqi Journal of Chemical and Petroleum Engineering*, **2025**, 26(1), 23-34.
[40] Tshangana, C., Muleja, A. Graphene oxide quantum dots membrane: A hybrid filtration-advanced technology system to enhance process of wastewater reclamation. *Chemical Papers*, **2024**, 78(2), 1317-1333.

Use your device to scan and read the article online

HOW TO CITE THIS ARTICLE
M. Arzaq, M. Az-Harry, H.A. Putri, N.H. Nasrul, S. Mulyati, C.M. Rosnelly, N.U. Barambu, M.P. Aulia, N. Arahman, High-Performance PES Membranes Prepared by VNIPS: Role of Brij-58 in Enhancing Surface Hydrophilicity and Antifouling Resistance. *Chem. Methodol.*, 2026, 10(5) 514-528
DOI: https://doi.org/10.48309/chemm.2026.562772.2051
URL: https://www.chemmethod.com/article_239830.html